Catalysis Today xxx (2015) xxx–xxx

Contents lists available at ScienceDirect

Catalysis Today

journal homepage: www.elsevier.com/locate/cattod

Activity study of NiO-based oxygen carriers in chemical looping steam methane reforming

Andy Antzara[a], Eleni Heracleous[b,c], Lishil Silvester[d], Dragomir B. Bukur[d,e], Angeliki A. Lemonidou[a,c,*]

[a] Department of Chemical Engineering, Aristotle University of Thessaloniki, University Campus, University Box 425, 54124 Thessaloniki, Greece
[b] School of Science & Technology, International Hellenic University (IHU), 14th km Thessaloniki–Moudania, 57001 Thessaloniki, Greece
[c] Chemical Process and Energy Resources Institute, Center of Research and Technology Hellas, CPERI/CERTH, 6th km Charilaou-Thermi Road, P.O. Box 361, 57001 Thessaloniki, Greece
[d] Chemical Engineering Program, Texas A and M University at Qatar, P.O. Box 23874, Doha, Qatar
[e] Artie McFerrin Department of Chemical Engineering, Texas A and M University, 3122 TAMU, College Station, TX 77843, United States

ARTICLE INFO

Article history:
Received 29 July 2015
Received in revised form 7 October 2015
Accepted 19 October 2015
Available online xxx

Keywords:
Oxygen transfer materials
Nickel oxide
Support
Nickel aluminate
Alumina
Silica
Titania
Zirconia
Chemical looping steam methane reforming
Hydrogen

ABSTRACT

This study evaluates the performance of NiO-based oxygen carriers supported on ZrO_2, TiO_2, SiO_2, Al_2O_3 and $NiAl_2O_4$ as conventional reforming catalysts at low temperature (650 °C) as well as oxygen transfer materials (OTMs) for chemical looping steam methane reforming. Conventional reforming experiments with pre-reduced OTMs demonstrated satisfactory performance of NiO/Al_2O_3, NiO/ZrO_2 and $NiO/NiAl_2O_4$ at 650 °C, with less than 8% relative decrease in conversion after 10 h time-on-stream. On the other hand, NiO/SiO_2 and NiO/TiO_2 were found to have low activity (<50% initial CH_4 conversion) and deactivated rapidly, eventually dropping to less than 10% CH_4 conversion after 2 h on stream. The three most promising materials were tested under chemical looping steam methane reforming conditions for twenty consecutive redox cycles in a fixed bed flow unit. NiO/ZrO_2 exhibited good activity with initial CH_4 conversion higher than 80% and had very good stability. Deactivation was minimal after 20 consecutive redox cycles, corresponding to 20 h exposure to CH_4/steam. NiO/Al_2O_3 and $NiO/NiAl_2O_4$ demonstrated similar high initial activity, but also high deactivation, leading to methane conversion of 59 and 63% conversion respectively at the end of the test.

1. Introduction

Hydrogen is an important raw material with wide use in the chemical and petrochemical industry. The current industrial major technology for large scale production of hydrogen is steam reforming of natural gas, which although a mature process, still remains very energy intensive. This thermodynamically limited reaction is industrially operated at temperatures higher than 800 °C in the presence of supported nickel-based catalysts [1]. High operating temperatures negatively affect the economic and environmental performance of the process, due to requirements for expensive materials such as high alloy nickel–chromium steel for the tubular reformer, irreversible carbon formation in the reactor, high energy consumption and CO_2 emissions resulting from demands of strongly endothermic reforming reaction [2]. It becomes therefore a necessity to introduce new environmentally friendly, low-energy consumption technologies with high hydrogen efficiency. In this context, research efforts have focused on new concepts for hydrogen production that operate at milder conditions and have lower carbon footprint, such as membrane assisted reforming [3–5], sorption enhanced reforming (SER) [6–9] and chemical looping reforming (CLR) [10–15].

Chemical looping methane reforming provides a novel route mainly for syngas production. It is based on the same principles as chemical looping combustion (CLC) [16–18] where the fuel is oxidized by oxygen provided by a solid oxygen transfer material (OTM) instead of direct mixing with air. The chemical looping system mainly consists of two interconnected fluidized bed reactors (an air reactor and a fuel reactor) with the oxygen transfer material circulating between the two. The OTM, typically a metal oxide, is reduced by the fuel in the first reactor and is then reoxidized by air in the second reactor. In the case of chemical looping reforming, the CH_4/OTM ratio is kept high in order to favor partial rather

* Corresponding author at: Department of Chemical Engineering, Aristotle University of Thessaloniki, University Box 425, 54124 Thessaloniki, Greece.
E-mail address: alemonidou@cheng.auth.gr (A.A. Lemonidou).

http://dx.doi.org/10.1016/j.cattod.2015.10.027
0920-5861/

than total oxidation of the fuel, leading to CO/H_2 production. In order to shift the product of the reaction to H_2, a hybrid chemical reforming process with steam or CO_2 addition has been proposed. In this case, the hydrogen yield increases due to the additional occurrence of reforming reactions in the fuel reactor. This however also increases the thermal demands of the process – since the reforming reactions are endothermic – and therefore low H_2O/C or CO_2/C ratios are preferred [19]. Taking this a step further, the combination of chemical looping steam methane reforming with sorption enhanced reforming in a single process has been suggested to further enhance hydrogen production, reduce the energy requirements of the process and produce a ready for sequestration CO_2 stream [19,20]. In the combined process, the OTM is mixed with a CaO-based CO_2 sorbent material that captures in situ the produced CO_2 and drives the equilibrium of reactions to the product side, resulting in increased H_2 yield and purity. The exothermic CaO carbonation provides in situ the necessary heat for the endothermic reactions in the fuel reactor, while the heat released by the highly exothermic OTM reoxidation in the second reactor is utilized for regeneration of the saturated CO_2 sorbent, minimizing the total requirements of the overall process. Therefore in order to efficiently transfer the heat from the OTM to the sorbent and maintain a low amount of solids circulating between the two reactors, which results in reduction to the overall operating cost of this novel process, the OTM should have a high enough Ni loading. Our recent thermodynamic-based calculations on the combined sorption enhanced chemical looping steam reforming process showed that a decrease of up to 55% of energy demands is possible compared to conventional steam reforming [20].

One of the challenges in chemical looping processes is the identification of effective oxygen transfer materials. A suitable oxygen carrier should be able to undergo multicycle redox reactions at intermediate to high operating temperatures and have sufficiently high oxygen transport capacity, high mechanical strength, low tendency for fragmentation, attrition and agglomeration and low production cost. Different metal oxides have been proposed in literature as possible candidates, such as CuO, NiO, Fe_2O_3 and CoO [21–25]. NiO appears to be the most promising for reforming processes, due to the excellent catalytic properties of reduced Ni for steam methane reforming and water gas shift reactions [24,26,27]. Even though NiO has a high oxygen transfer capacity, it exhibits poor re-oxidation over multiple reduction and oxidation cycles in bulk form due to nickel agglomeration, which affects its cyclic performance and renders it unsuitable for chemical looping applications. Therefore, NiO is commonly supported on refractory oxides for increased stability. Among the supporting inert materials, Al_2O_3 has received the highest attention due to its high thermal and mechanical strength and favorable fluidization properties [28–30]. However in NiO–Al_2O_3 systems there is always formation of mixed $NiAl_2O_4$, a resilient phase that reduces at temperatures above 850 °C, "neutralizing" a significant fraction of NiO. De Diego et al. [26] reported results from evaluation of Ni-based OTMs supported on different types of alumina in a TGA and in a batch fluidized bed reactor unit. It was shown that the type of alumina (α-, γ- and θ-Al_2O_3) affects the reducibility of NiO by methane, with NiO on γ-Al_2O_3 demonstrating the lowest activity due to extensive formation of $NiAl_2O_4$. Better results were obtained with the lower surface areas α- and θ-aluminas. Only a few studies have utilized other types of supports, such as SiO_2, TiO_2 or ZrO_2 [22,29,31,32].

In the previous study [33], we performed preliminary evaluation of NiO supported on alumina and zirconia as potential OTMs for chemical looping steam methane reforming. NiO supported on ZrO_2 exhibited very stable redox behavior during twenty CH_4 reduction/air oxidation cycles with almost complete reduction of NiO to metallic Ni in every cycle (94%). In contrast, a low degree of reduction was obtained initially with NiO/Al_2O_3 (51%) which however gradually increased to 85% during the first eight cycles and then remained stable during the remaining twelve cycles. It was postulated that the cyclic reduction/oxidation of the material leads to restructuring of the surface and reduction of a $NiAl_2O_4$ species that form during re-oxidation of the reduced OTM. In this work, we extend our study by investigating the effect of additional three supports (SiO_2, TiO_2 and $NiAl_2O_4$), focusing on extensive testing of all materials in a fixed bed flow unit under conventional reforming and multiple chemical looping steam methane reforming cycles. Reaction tests have been complemented by detailed characterization of physicochemical properties of the OTMs before and after reaction to identify crucial properties that determine their performance in the targeted reaction.

2. Experimental

2.1. Preparation of oxygen carriers

NiO oxygen carriers with a constant loading of 40 wt% of NiO supported on commercial Al_2O_3, SiO_2, TiO_2 and ZrO_2 (Saint Gobain-NORPRO) and one lab-synthesized $NiAl_2O_4$ were prepared via wet impregnation. For the preparation of the $NiAl_2O_4$ support, a co-precipitation method was followed. Stoichiometric amounts of $Ni(NO_3)_2{\cdot}6H_2O$ (Merck) and $Al(NO_3)_3{\cdot}9H_2O$ (Panreac) were dissolved in distilled H_2O and were stirred at room temperature until a transparent green solution was obtained. A 1 M NH_4OH solution was added dropwise until the pH reached ~8 and the precipitation occurred. The precipitate particles were then filtered, washed with distilled water and dried overnight at 100 °C. Calcination of the dried powder was performed at 900 °C for 11 h in air flow.

For the preparation of the NiO-supported OTMs, the supports were first crushed and sieved in order to obtain a particle size of $100 < d_p < 500$ μm. Nickel nitrate ($Ni(NO_3)_2{\cdot}6H_2O$, Merck) was used as a precursor salt. The required amount of precursor in order to achieve 40 wt% NiO loading was dissolved in de-ionized water and was mixed with the appropriate amount of support in a round bottom flask. The mixture was heated slowly in a rotary evaporator for 1 h under stirring at 70 °C. The solvent was then evaporated at 80–85 °C under reduced pressure. The solids were dried overnight at 100 °C and were calcined at 650 °C for 4 h in air flow.

2.2. Characterization of oxygen carriers

Surface areas and pore volumes of the samples were determined by N_2 adsorption at 77 K, using the multipoint BET analysis method, with an Autosorb-1 Quantachrome flow apparatus. Prior to the measurements, the samples were dehydrated in vacuum at 250 °C overnight.

X-ray diffraction (XRD) patterns were obtained with a Siemens D500 diffractometer and Cu-Kα radiation with radiation wavelength of 0.15406 nm. An aluminum holder was used to support the samples during the measurements. The intensity data were collected over a 2θ range of 5–80° with a step of 0.04° and a scanning rate of 2 s/point. The crystallite size of metallic Ni in used samples was determined from the XRD patterns, using the Debye–Scherrer's equation:

$$D = \frac{0.64 * \lambda}{(\beta - \beta_0)[\cos(\theta)]} \quad (1)$$

where D is the crystallites size (nm), λ the radiation wavelength (Cu-Kα, $\lambda = 0.15406$ nm), β is the full width at half of the maximum of the peak (radians), β_0 is an appropriate correction for the peak broadening due to the diffractometer itself ($\beta_0 \approx 0.129°$) and θ is the angular position of the peak. Fitting of the peaks was performed using Lorentzian function. In order to have more accurate results only the two high intensity peaks of Ni at 44.4° and 51.8°

Please cite this article in press as: A. Antzara, et al., Activity study of NiO-based oxygen carriers in chemical looping steam methane reforming, Catal. Today (2015), http://dx.doi.org/10.1016/j.cattod.2015.10.027

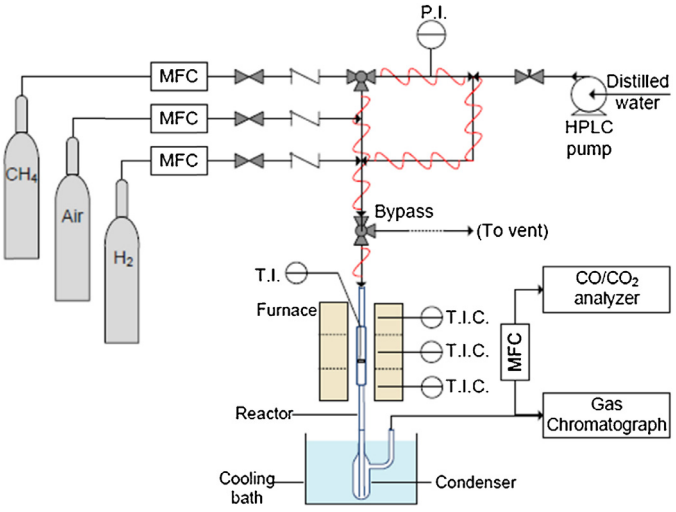

Fig. 1. Schematic layout of the fixed bed bench-scale flow unit.

2θ positions were used, while the low intensity Ni peak at 76.4° was excluded from the calculations of the average crystallite size in order to minimize the errors related to non-proper fitting.

H_2-temperature programmed reduction was performed for all materials in an AutoChem II 2920 unit equipped with a thermal conductivity detector (TCD). Prior to the measurements, the samples were pre-treated in air up to 650 °C to ensure that they were in fully oxidized form. Temperature was then lowered to room temperature (RT) in He flow. Temperature programmed reduction from RT to 1000 °C was performed with a heating rate of 10 °C/min under 10% H_2/Ar flow and maintaining the final temperature of 1000 °C for 30 min.

Temperature Programmed Oxidation (TPO) experiments were performed in a specially designed lab scale flow unit coupled with a mass analyzer (Omnistar GSD 320) in order to determine the amount of coke deposited on the materials after reaction. The used sample was loaded in a U-shaped quartz reactor, equipped with a coaxial thermocouple for temperature monitoring. The sample was initially pretreated for 30 min at 250 °C under He flow followed by cooling to room temperature. TPO was performed under a flow of 20% O_2/He with a heating rate of 10 °C/min from RT to 900 °C. The outlet gas composition was monitored online with the mass spectrometer analyzer. Quantitative analysis of the evolved CO_2 was based on (m/z) 44.

In order to determine the surface oxidation state of Ni after reforming, the NiO oxygen carriers were characterized by XPS. Characterization of the fresh samples after reduction in H_2 at 650 °C for 1 h was also conducted for comparison. The XPS measurements were performed with a Kratos Analytical AXIS ultra DLD instrument equipped with a monochromatic Al X-ray source. XPS spectra were recorded with pass energy 20 eV, step 0.1 eV and X-ray power 150 W. Deconvolution of the peaks was performed with a Kratos Vision software (Version 2.2.10) using Shirley background subtraction and mixed Gaussian–Lorentzian functions. Binding energies were referenced to C 1s at 284.6 eV.

2.3. Evaluation of conventional and chemical looping steam reforming activity in a flow unit

The evaluation of the NiO-OTMs' conventional and chemical looping steam reforming activity was performed at atmospheric pressure in a bench scale laboratory flow unit. The unit consists of liquid and gas feed section, a fixed bed reactor and the product analysis section (Fig. 1). The incoming gases are controlled by mass flow controllers and are pre-mixed before entering the reactor. An Ultra-Fast Liquid Chromatography (UFLC) pump (Shimadzu) is used for admission of distilled water (steam) to the reactor through a pre-heater. The fixed bed quartz reactor (10 mm internal diameter), with a coaxial thermocouple for temperature monitoring, is heated electrically by a tubular furnace, with three independently controlled temperature zones. A fritted quartz disk placed in the center of the reactor is used to hold the catalytic bed. Gaseous products exiting the reactor are cooled to condensate the unreacted steam and the gas phase products are analyzed with an online gas chromatograph (Agilent Technologies, 7890A) equipped with thermal conductivity detector. Two columns (Molecular Sieve and Poraplot) in series by pass configuration are used for the analysis of the outlet gas stream. The Molecular Sieve column is used for separation of H_2, CH_4 and CO, while the Poraplot column is used for detection of CO_2. The CO and CO_2 concentrations in the reactor exit are also monitored by a gas analyzer (Madur, Mamos-200).

Table 1
Textural properties of the five 40 wt% NiO OTMs and the pure supports.

	BET surface area (m^2/g)	Pore volume (cm^3/g)
Al_2O_3	203	0.58
40% NiO/Al_2O_3	117	0.33
ZrO_2	93	0.28
40% NiO/ZrO_2	22	0.15
SiO_2	100	0.47
40% NiO/SiO_2	55	0.27
TiO_2	39	0.31
40% NiO/TiO_2	16	0.15
$NiAl_2O_4$	81	0.27
40% NiO/$NiAl_2O_4$	50	0.19

For the evaluation of the conventional steam reforming activity of the OTMs, about 50 mg of material diluted with a predetermined amount of quartz particles was loaded in the reactor. The amount of diluent varied between 55 and 75% of the weight of the OTM, based on the specific density of each material, in order to achieve a catalytic bed of constant length over all materials and a Gas Hourly Space Velocity of 100,000 h^{-1}. The sample was initially heated to 650 °C under He flow, followed by in situ reduction in 33% H_2/He for 1 h at 650 °C in order to obtain the metallic form of nickel. After the reduction, reforming was performed by switching to CH_4 and steam flow, with S/C molar ratio of 3. The reaction was conducted isothermally at 650 °C for 10 h.

For the evaluation of the chemical looping steam reforming activity, about 50 mg of material diluted with a predetermined amount of quartz particles (in order to maintain the Gas Hourly Space Velocity constant at 100,000 h^{-1}) was loaded in the reactor. The materials were initially exposed to CH_4/steam in their oxidized state for 1 h at 650 °C (S/C ratio of 3). During the first 10 min of the reduction/reforming step a small external H_2 flow (5% of the total flow) was added in order to facilitate NiO reduction. After 1 h, the temperature of the reactor was raised to 850 °C under He flow and then the feed was switched to air for re-oxidation for 20 min and the cycle was then repeated.

The performance of the OTMs is expressed in terms of CH_4 conversion (X_{CH_4}) which was calculated with the following equation:

$$X_{CH_4}\ (\%) = \frac{CO_{out} + CO_{2,out}}{CH_{4,out} + CO_{out} + CO_{2,out}} \times 100 \quad (2)$$

3. Results and discussion

3.1. Characterization of oxygen carriers

The surface area and pore volume of the NiO supported oxygen carriers, along with those of the pure supports, are presented in Table 1. Upon impregnation of the supports with NiO, both the

Please cite this article in press as: A. Antzara, et al., Activity study of NiO-based oxygen carriers in chemical looping steam methane reforming, Catal. Today (2015), http://dx.doi.org/10.1016/j.cattod.2015.10.027

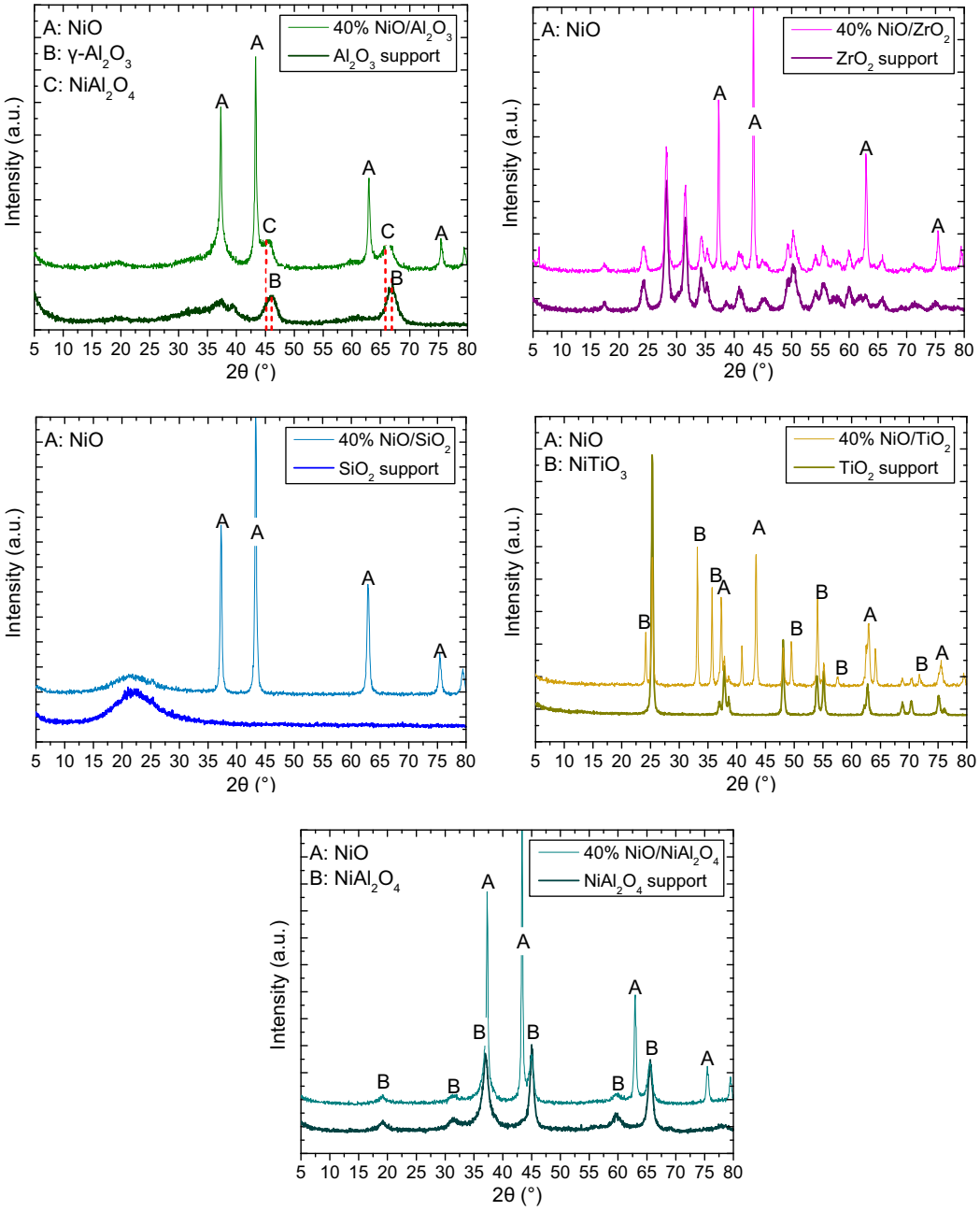

Fig. 2. XRD patterns of 40% NiO supported OTMs and respective pure supports.

surface area and the pore volume decreased. Considering the high NiO loading (40 wt%), it can be deduced that for the Al_2O_3, SiO_2 and $NiAl_2O_4$ supported OTMs the decrease in surface area is almost exclusively due to the replacement of the high surface area of the supports with NiO. In the case of zirconia and titania supports, the reduction in surface area is much higher, indicating blockage of the pores by NiO and/or poor stability of the supports under the high temperature calcination conditions.

The X-ray diffraction patterns of calcined OTMs and the respective as received pure supports are shown in Fig. 2(a)–(e). In the case of the alumina supported OTM, the presence of both NiO and the mixed nickel aluminate ($NiAl_2O_4$) crystal phases is evident, indicating a strong interaction between alumina and nickel oxide. Similar results are obtained for titania, where formation of $NiTiO_3$ is observed. On the contrary, only the pure NiO crystal phase is detected when ZrO_2 and SiO_2 are used as supports. Therefore, interaction between these refractory oxides and nickel oxide can be characterized as rather weak. The diffractogram of the synthesized $NiAl_2O_4$ support displays high intensity peaks of the pure nickel aluminate phase, indicating successful preparation. The highly crystalline nature of this support differentiates $NiAl_2O_4$ from the nearly amorphous alumina support, as well as the other low crystallinity refractory oxides used. The $NiO/NiAl_2O_4$ oxygen transfer material exhibits clear diffractions attributed to NiO, in addition to those of $NiAl_2O_4$.

The reducibility of the NiO oxygen carriers supported on different oxides was investigated by H_2 temperature programmed reduction and the TPR profiles are presented in Fig. 3. NiO/Al_2O_3 exhibits two main peaks with a maximum at 322 °C and 729 °C. The first peak is ascribed to the reduction of NiO without or with low interaction with the support to Ni^0 metal phase [34,35]. The second peak at ~730 °C is attributed to the reduction of nickel in $NiAl_2O_4$ [36–38],

Please cite this article in press as: A. Antzara, et al., Activity study of NiO-based oxygen carriers in chemical looping steam methane reforming, Catal. Today (2015), http://dx.doi.org/10.1016/j.cattod.2015.10.027

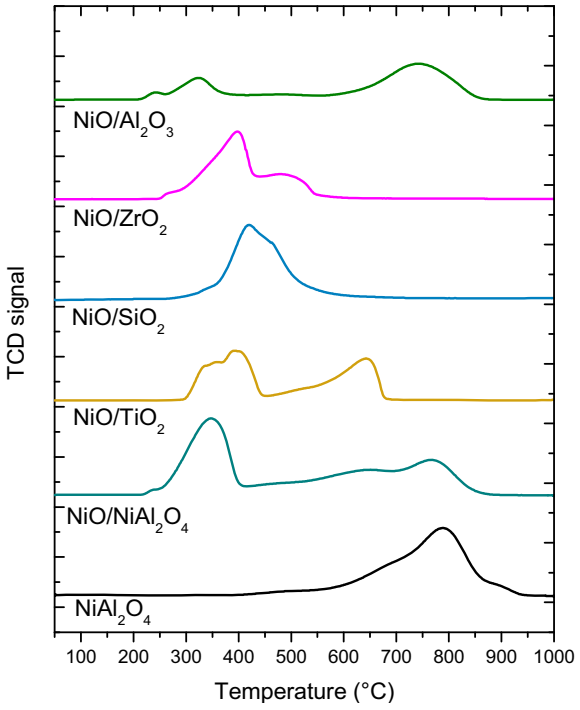

Fig. 3. H_2 temperature-programmed reduction profiles for the five NiO-OTMs and $NiAl_2O_4$ support.

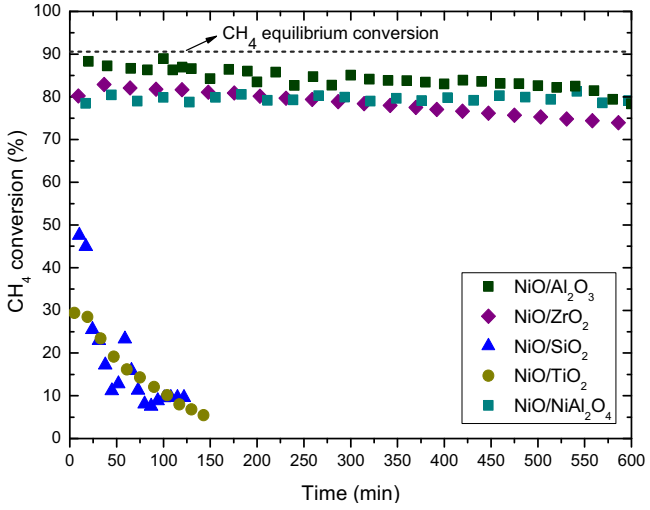

Fig. 4. Methane conversion as a function of time for supported NiO oxygen carriers (T = 650 °C, S/C ratio = 3, GHSV = 100,000 h^{-1}).

confirming the XRD findings that indicate that part of NiO is bound in the nickel aluminate phase. Compared with the TPR profile of the as-synthesized pure $NiAl_2O_4$ support, nickel aluminate on alumina reduces at ~70 °C lower temperature. This could be due to the co-existence of nickel aluminate with "free" NiO in the NiO/Al_2O_3 OTM. Li and Chen [38] observed that in a series of NiO/Al_2O_3 catalysts the reduction of nickel aluminate shifted to lower temperatures with increasing NiO loading. This was attributed to the presence of more easily reducible NiO species that may facilitate nucleation of other Ni nuclei that could originally interact strongly with the support, thus enhancing the reduction of these more strongly interacting NiO species. On the contrary the $NiAl_2O_4$ peak in the TPR profile of the $NiO/NiAl_2O_4$ OTM appears at higher temperature (~780 °C). In addition, the shift of the NiO reduction peak to higher temperature and the shoulder at 625 °C indicate a stronger interaction between free NiO and the $NiAl_2O_4$ compared to γ-Al_2O_3 support. The reduction profile of NiO/TiO_2 presents similar features, with two low temperature peaks at 362 and 394 °C, attributed to NiO reduction that has different degree of interaction with the titania surface and a high temperature one ascribed to the reduction of bulk $NiTiO_3$ to Ni^0 [39,40]. In the presence of TiO_2, NiO seems to reduce at a higher temperature than on Al_2O_3 (394 °C vs 322 °C). $NiTiO_3$ on the other hand is reduced at lower temperatures than $NiAl_2O_4$, pointing out to a weaker interaction of NiO with TiO_2. This is also supported by the fact that the peak attributed to the reduction of free NiO has higher intensity in TiO_2 than in Al_2O_3 and shows that more NiO is reducible at low temperatures on titania. NiO/SiO_2 demonstrates only one large reduction peak with a maximum at 415 °C due to the reduction of NiO to Ni metal. Although the XRD of NiO/ZrO_2 showed the presence only of NiO, the TPR profile presents two clear reduction peaks at 394 °C and 474 °C. The reduction peak at low temperature corresponds to bulk NiO with low interaction with the support, while the reduction peak at higher temperature could be attributed to the fixed NiO interacting with (but not chemically bonded to) the ZrO_2 support. In summary, the temperature for free NiO reduction to metallic Ni^0 decreases in the order; $SiO_2 > ZrO_2 = TiO_2 > Al_2O_3$. These differences could be attributed to the different interaction of the "free" NiO with the individual supports as well as to different extent of sintering of nickel oxide at the high calcination temperature, which may significantly account for the shift of the maximum reduction temperature of these NiO species [41].

3.2. Performance evaluation in conventional steam methane reforming

3.2.1. Activity testing

For an oxygen carrier to be suitable for use in chemical looping steam methane reforming, it is a prerequisite for the material to exhibit good reforming activity in its reduced form. Therefore, the materials were pre-reduced in situ and were then tested as conventional reforming catalysts in steam methane reforming at 650 °C with S/C ratio of 3. It should be noted that the developed oxygen transfer materials were tested at relatively low temperature (650 °C), as we intend to use them in the combined chemical looping reforming process with in situ CO_2 capture with CaO-based sorbents [20,42]. Based on a recent thermodynamic analysis of the sorption enhanced chemical looping reforming process performed by our group [20], the optimum temperature for effective CO_2 capture by CaO-based sorbents is ~650 °C. In Fig. 4, methane conversion is plotted as a function of time-on-stream for the five oxygen carriers. The Ni catalysts supported on titania and silica have low activity; initial CH_4 conversion is low (less than 50% CH_4 conversion) and decreases rapidly, eventually dropping below 10% CH_4 conversion after less than 2 h on stream.

On the other hand, NiO/ZrO_2, NiO/Al_2O_3 and $NiO/NiAl_2O_4$ have a satisfactory activity, with high initial methane conversion ranging from 80 to 87%. Both NiO/Al_2O_3 and NiO/ZrO_2 were relatively stable with approximately 8% relative decrease in conversion after 10 h on stream. $NiO/NiAl_2O_4$ OTM had lower initial activity (~80% conversion) compared to NiO/Al_2O_3, but it exhibited the highest stability with almost no deactivation. After 10 h of testing it had the same conversion as NiO/Al_2O_3 OTM. It seems that the use of $NiAl_2O_4$ as support stabilizes the surface metallic nickel species. During the reduction of the OTM by H_2, two types of metallic nickel can be formed: "free" metallic nickel by the reduction of NiO and fixed monodispersed nickel species produced by the partial reduction of $NiAl_2O_4$. These latter species consist of nickel particles located in the nickel aluminate structure that are stabilized by the surrounding environment, preventing sintering and reoxidation that could lead to the loss of activity [43].

Please cite this article in press as: A. Antzara, et al., Activity study of NiO-based oxygen carriers in chemical looping steam methane reforming, Catal. Today (2015), http://dx.doi.org/10.1016/j.cattod.2015.10.027

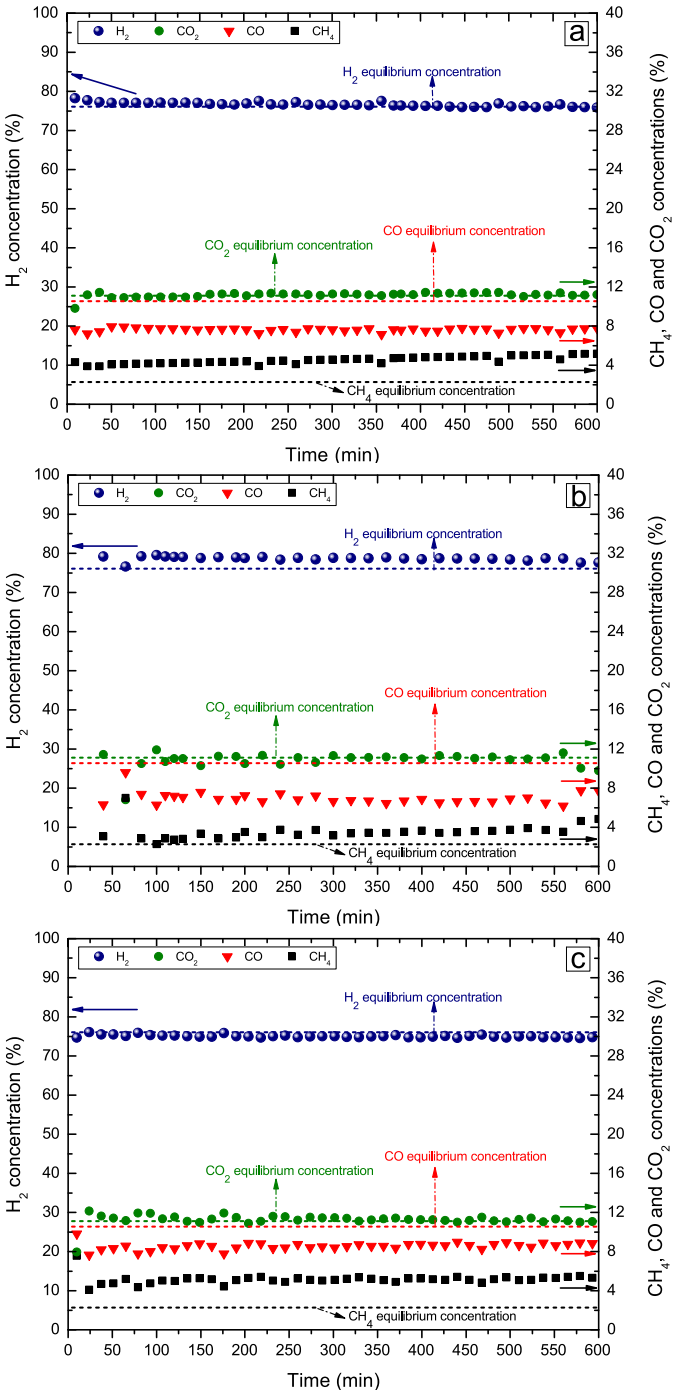

Fig. 5. Product concentration as a function of time for (a) NiO/ZrO_2, (b) NiO/Al_2O_3 and (c) $NiO/NiAl_2O_4$ (T = 650 °C, S/C ratio = 3, GHSV = 100,000 h^{-1}).

Analysis of the reaction products as a function of time on stream is presented only for the three most active catalytic materials. The composition of the outlet dry product stream from methane reforming over NiO/ZrO_2, NiO/Al_2O_3 and $NiO/NiAl_2O_4$ is shown in Fig. 5(a)–(c) respectively. High concentration of hydrogen, in the order of 75–80% and near the equilibrium, is observed with all materials. The concentration of CO remains in all cases at low levels, while CO_2 concentration is in 10–12% range. The low levels of CO, much lower than the equilibrium predicted concentration, indicate that the materials are also active in the water gas shift reaction. As shown in Fig. 5(a)–(c), the concentration of CO and CO_2 in the outlet stream of the reactor is stable with

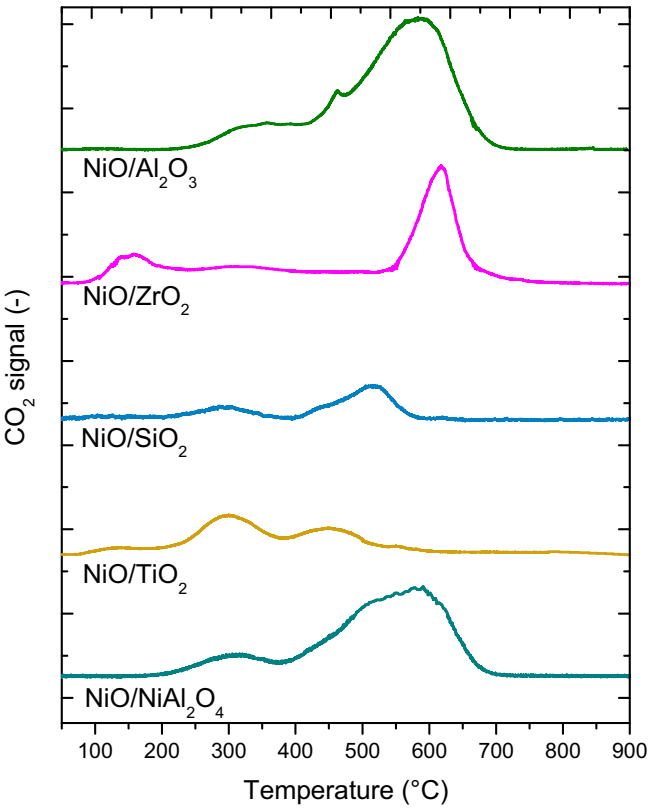

Fig. 6. Temperature-programmed oxidation profiles of spent catalysts.

time-on-stream throughout the entire experiment for all supported NiO-OTMs. On the other hand methane concentration increases with time for NiO/ZrO_2 and NiO/Al_2O_3, reflecting the slow decrease of methane conversion with time-on-stream, whereas it remains stable for $NiO/NiAl_2O_4$ which exhibited the highest stability. The opposite trend is observed for H_2 concentration; as methane conversion decreases due to catalyst deactivation, hydrogen production decreases as well.

3.2.2. Post-reaction characterization

The pure reforming experiments demonstrated that the support has a strong influence on the performance of NiO OTMs. The use of ZrO_2, Al_2O_3 and $NiAl_2O_4$ as supports led to the synthesis of OTMs with high catalytic activity and stability in conventional methane reforming to hydrogen with satisfactory stability, while on the other hand TiO_2 and SiO_2 supports demonstrated low initial methane conversion and very high deactivation rate. Possible reasons for the high deactivation could be either partial re-oxidation of the metallic Ni phase to NiO by steam, extensive coke deposition [44,45] or significant sintering of the Ni particles on the carrier surface [46,47]. To investigate the above possibilities, post-characterization of the NiO supported samples after the reforming reaction was performed with TPO (for coke determination), XRD (for determining the Ni crystal size) and XPS (for Ni oxidation state determination).

TPO profiles of the spent catalysts are presented in Fig. 6, while the amount of deposited coke and the rate of carbon production expressed in moles of C per mol of CH_4 in the inlet of the reactor are given in Table 2. All materials exhibited two CO_2 peaks, indicating the formation of two types of carbon: one oxidized at low temperatures (300 °C), probably corresponding to absorbed CHx or oligomeric carbon that can be easily removed by H_2 or steam under reaction conditions, and one at higher temperatures corresponding to the oxidation of polymeric carbon [47–49]. NiO/TiO_2 and

Please cite this article in press as: A. Antzara, et al., Activity study of NiO-based oxygen carriers in chemical looping steam methane reforming, Catal. Today (2015), http://dx.doi.org/10.1016/j.cattod.2015.10.027

Table 2
Carbon deposition and rate of carbon production for the five spent NiO-OTMs.

	Time on stream (h)	wt% C on catalyst	Rate of C production [mol $C_{(s)}$/mol CH_4 in] (%)
40% NiO/SiO_2	2	0.003	0.49
40% NiO/TiO_2	2	0.025	0.56
40% NiO/ZrO_2	10	0.020	0.07
40% NiO/Al_2O_3	10	0.087	0.29
40% $NiO/NiAl_2O_4$	20	0.231	0.39

Table 3
Crystal size of reduced fresh and spent NiO/SiO_2 and NiO/TiO_2 calculated from XRD patterns.

Sample	Crystal size (nm)
40% NiO/SiO_2	
Fresh	28.0
Used	41.4
40% NiO/TiO_2	
Fresh	38.7
Used	48.1

NiO/ZrO_2 also had small peaks at very low temperature (<200 °C), corresponding to loosely bound carbon, however they are much smaller than the higher temperature peaks. The relative amount of each type of carbon varies greatly depending on the support used. In the case of NiO/Al_2O_3, NiO/ZrO_2 and $NiO/NiAl_2O_4$ the main CO_2 peak occurs at temperature around 600 °C. On the other hand, the amount of easily removed carbon is much higher over NiO/TiO_2, while over NiO/SiO_2 the two peaks are comparable.

Comparing the total amount of carbon deposited on the catalyst surface (Table 2), very low values were observed for all samples, with $NiO/NiAl_2O_4$ demonstrating the highest amount of formed coke (0.231 wt%). As the exposure of each material to reaction conditions (CH_4/steam atmosphere) was different, carbon deposition values are also presented as the rate of coke formation per unit of CH_4 feed. The corrected carbon formation rates show that Ni supported on SiO_2 and TiO_2 exhibits the highest rates of carbon production, followed by Ni on $NiAl_2O_4$, Al_2O_3 and finally ZrO_2. Even though the use of SiO_2 and TiO_2 support seems to enhance the deposition of carbon on the catalyst surface, the differences are not significant enough to provide explanation for their poor performance in the reforming reaction.

In order to detect whether Ni agglomeration occurs during reforming, the crystal size of metallic nickel on NiO/SiO_2 and NiO/TiO_2, fresh after reduction in H_2 and used after the reforming reaction, was calculated form XRD patterns. Comparing the average crystal size of fresh and used catalysts (Table 3), a small increase is observed probably due to the agglomeration of nickel crystallites during the reforming reaction. However the extent is very low to justify the differences in performance among the nickel OTMs supported on different oxides.

Reoxidation of Ni in the presence of excess steam at relatively low temperature reforming conditions has been previously reported [50,51]. X-ray Photoelectron Spectroscopy was employed to determine whether the origin of fast deactivation for the materials supported on titania and silica is the re-oxidation of metallic Ni to inactive-to-reforming NiO by steam during the reaction. XPS characterization was performed on a representative low stability material, NiO/TiO_2, fresh pre-reduced in H_2 and after the reforming experiments. The same characterization was also performed on NiO/ZrO_2 samples, reduced and after reaction, to be used as benchmark, considering that this material exhibited high activity and stability in the reforming reaction. The Ni 2p spectra of fresh NiO/TiO_2 and NiO/ZrO_2 in reduced form are presented in Fig. 7a and b respectively. Two main peaks centered on 852.2 eV and 854.7 eV are observed in the $2p_{3/2}$ transition of nickel on NiO/TiO_2, corresponding to metallic Ni and NiO respectively. The satellite peak of NiO also appears at ~659.5 eV [52,53]. Similar peaks are

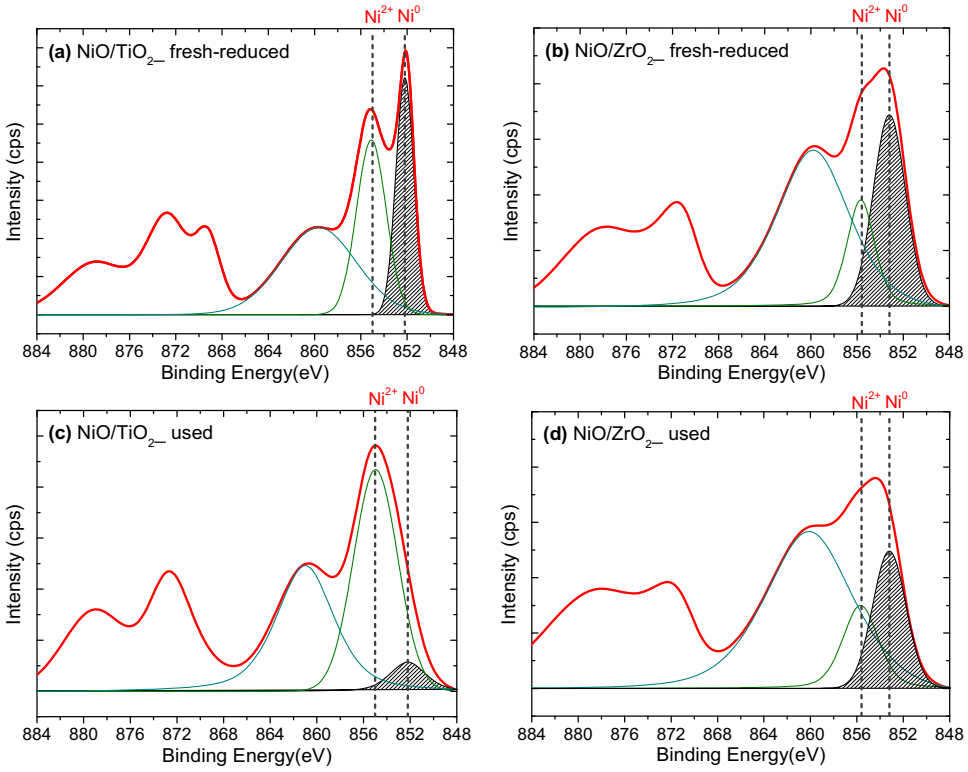

Fig. 7. X-ray photoelectron spectra of Ni 2p transition of the fresh reduced NiO/TiO_2 (a) and NiO/ZrO_2 (b) and the NiO/TiO_2 (c) and NiO/ZrO_2 (d) after conventional reforming experiments.

Please cite this article in press as: A. Antzara, et al., Activity study of NiO-based oxygen carriers in chemical looping steam methane reforming, Catal. Today (2015), http://dx.doi.org/10.1016/j.cattod.2015.10.027

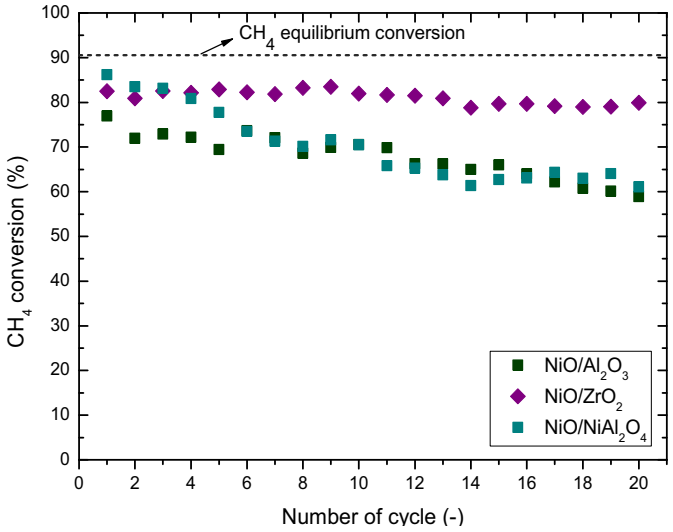

Fig. 8. Methane conversion during 20 reduction-reforming/oxidation cycles for NiO supported on Al_2O_3, ZrO_2 and $NiAl_2O_4$ (*Reduction/reforming*: $T = 650\,^{\circ}C$, S/C ratio = 3, GHSV = 100,000 h^{-1}, duration: 1 h, *Oxidation*: $T = 850\,^{\circ}C$, air flow, duration: 15 min).

also detected in the Ni 2p spectrum of NiO/ZrO_2, shifted however to slightly higher binding energies (853 eV, 855.3 eV and 860.1 eV respectively), implying a different electronic density of nickel on the surface of zirconia. Even though these samples were reduced prior to XPS measurements, peaks corresponding to NiO appear in the spectra with 54% and 36% contribution to the total nickel content in NiO/TiO_2 and NiO/ZrO_2 respectively. This indicates that part of surface Ni is re-oxidized by ambient air, as the XPS measurements were performed ex situ.

The corresponding XPS spectra of the used NiO/TiO_2 and NiO/ZrO_2 after the conventional reforming experiments are presented in Fig. 7c and d. For NiO/TiO_2, the comparison with the spectrum of the fresh catalysts in reduced form clearly portrays that in the used materials more than 90% of surface nickel appears in its oxidized state. This shows that metallic Ni is almost completely re-oxidized by steam during the reaction, leading to poor performance and fast deactivation. On the other hand, nickel on ZrO_2 seems to remain in its reduced state after reaction, with only ~45% of Ni being re-oxidized which is comparable to the part of Ni in the oxidized state in the fresh reduced sample (36%). The re-oxidation of nickel to nickel oxide by steam could also be a reason of deactivation of the NiO/SiO_2 sample [54,55]. In addition, it is known that silica is very unstable in the presence of steam which leads in hydrolysis and total restructuring of the support, resulting in large decrease of pore volume and surface area [56]. Unfortunately, it was not possible to measure the BET surface area and pore volume of the used samples due to the low quantity of sample employed in the conventional reforming experiments.

3.3. Chemical looping reforming experiments

Based on the evaluation of the OTMs under conventional reforming conditions, NiO/Al_2O_3, NiO/ZrO_2 and $NiO/NiAl_2O_4$ in reduced form appear suitable for reforming, exhibiting high methane conversion and satisfactory stability. These materials were therefore selected for further testing under chemical looping steam methane reforming conditions, starting with the oxygen carriers in oxidized form. The OTMs chemical looping activity was evaluated during 20 redox cycles in a bench scale fixed bed flow unit.

Fig. 8 presents the conversion of CH_4 as a function of redox cycles for the three supported NiO oxygen carriers. All three OTMs exhibit high initial CH_4 conversion, ranging between 78 and 87%. These values are very similar to what was attained during the conventional reforming experiments, proving that nickel oxide can indeed be reduced in CH_4/steam atmosphere, yielding a metallic nickel surface of similar reforming activity with that obtained with hydrogen pre-reduction. However, the stability of OTMs was different under chemical looping conditions. Whereas $NiO/NiAl_2O_4$ was the most stable during conventional reforming, NiO/ZrO_2 exhibited by far higher stability (less than 2% relative conversion decrease) than either NiO/Al_2O_3 or $NiO/NiAl_2O_4$ in the chemical looping steam methane reforming tests. Deactivation of the two latter materials is similar and equal to ~23% activity loss after 20 consecutive redox cycles, corresponding to 20 h of exposure to CH_4/steam. This loss of activity could be attributed to low thermal stability of alumina and nickel aluminate supports when exposed to high temperature of re-oxidation (850 °C) for extended periods of time [55].

The reformate gas concentration during a representative redox cycle (5th cycle) are presented in Fig. 9(a), (b) and (c) for NiO/ZrO_2, NiO/Al_2O_3 and $NiO/NiAl_2O_4$ respectively. Symbols refer to data acquired from the gas chromatograph. CO and CO_2 concentrations recorded on-line by the gas analyzer are also presented in the same figures with continuous lines. A sharp evolution of the reformate gas directly after start-up indicates that the NiO readily reduces with a very fast rate, even in the presence of steam, over all supports. It also shows that the reforming reactions are catalyzed immediately as soon as a small amount of metallic nickel forms. The hydrogen that is produced from the reforming reactions helps further in completing the NiO reduction and maintaining the oxygen carriers in reduced form for the entire duration of the reforming cycle. Steady state conditions in the reactor are achieved after ~20 min of reaction time. High hydrogen concentrations (70–76%) are observed for all tested OTMs. Moreover, it is important to note that no CO_2 evolution was observed during the re-oxidation step (in any cycle) for the ZrO_2, Al_2O_3 or $NiAl_2O_4$ supported NiO, indicating that the use of high S/C ratio employed prevents carbon formation. Based on studies by Cho et al. [57] carbon formation on Ni-based particles can be hampered by adding 50 vol% steam to the fuel.

Comparison of our results with literature is difficult since most of the studies in chemical looping reforming employed very low S/C ratios [11,27,30,58] or used only CH_4 as feed. Dupont et al. [58] performed chemical looping steam methane reforming experiments at 800 °C with a S/C ratio of 1.8 using NiO-based OTMs with Ni loading ranging from 12.6 to 39.2% and observed high CH_4 conversion levels (99%) during the whole duration of the 10 min reforming step. These conversion levels are higher than the ones recorded in this study (80–85%), mainly due to thermodynamic limitations at the lower reforming temperature employed in our study.

The results from the evaluation of NiO/ZrO_2, NiO/Al_2O_3 and $NiO/NiAl_2O_4$ in cyclic chemical looping steam methane reforming experiments indicate that these oxygen carriers have good potential for use in sorption enhanced chemical looping reforming, especially NiO/ZrO_2 OTM. Similar performance as that attained during conventional reforming can be achieved with additionally good stability in alternating reforming/oxidation conditions. Process wise, the implementation of the sorption enhanced chemical looping reforming with these materials will lead to a process with significantly lower thermal demands than the conventional reforming process (up to 55% [20]), as the reforming reaction is performed at lower temperature and part of the required heat is generated by the OTM's reoxidation. Moreover, CO_2 is captured and separated in one-step, significantly simplifying the reforming process which is composed of the reformer, plus water gas shift reactors and separation processes. The actual impact of replacing a conventional reforming process with a sorption enhanced chemical looping reforming process in terms of process complexity and economic figures can only be assessed via a detailed techno-economic

Please cite this article in press as: A. Antzara, et al., Activity study of NiO-based oxygen carriers in chemical looping steam methane reforming, Catal. Today (2015), http://dx.doi.org/10.1016/j.cattod.2015.10.027

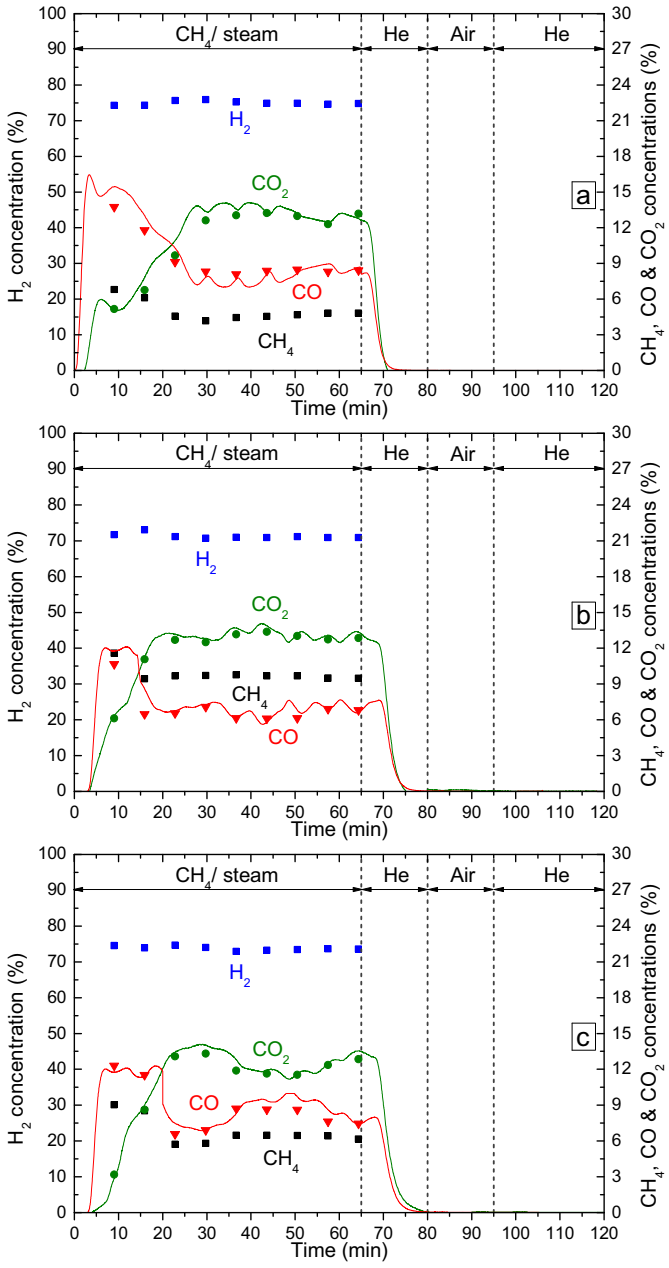

Fig. 9. Reformate gas concentration as a function of time during the 5th cycle for NiO/ZrO_2 (a), NiO/Al_2O_3 (b) and $NiO/NiAl_2O_4$ (c) (*Reduction/reforming*: $T = 650\,^{\circ}C$, S/C ratio = 3, GHSV = 100,000 h^{-1}, duration: 1 h, *Oxidation*: $T = 850\,^{\circ}C$, air flow, duration: 15 min).

analysis, but the outlook for the new process concept is positive in all aspects.

4. Conclusions

In this work, NiO-based oxygen carriers supported on ZrO_2, TiO_2, SiO_2, Al_2O_3 and $NiAl_2O_4$ were evaluated as oxygen transfer materials (OTMs) for chemical looping steam methane reforming. Conventional reforming experiments with pre-reduced materials showed that NiO/ZrO_2, NiO/Al_2O_3 and $NiO/NiAl_2O_4$ are highly active reforming catalysts even at the low temperature of $650\,^{\circ}C$. The materials exhibited initial methane conversions in the 80–87% range and less than 8% decrease in conversion after 10 h time-on-stream. On the other hand, NiO/SiO_2 and NiO/TiO_2 exhibited low initial activity and deactivated rapidly after less than 2 h on stream. Post-characterization of the used materials with XPS showed that the most probable reason for deactivation is oxidation of metallic nickel by steam to nickel oxide on the titania support, whereas nickel on NiO/ZrO_2 remains in reduced state.

NiO/ZrO_2, NiO/Al_2O_3 and $NiO/NiAl_2O_4$ were further tested under chemical looping steam methane reforming conditions for 20 consecutive cycles in a fixed bed flow unit. All three OTMs exhibited high initial CH_4 conversion, ranging between 78 and 87%, similar to that attained during conventional reforming. This result is important as it proves that nickel oxide can indeed be reduced in CH_4/steam atmosphere, yielding a metallic nickel surface of similar reforming activity as that obtained with hydrogen pre-reduction. Moreover, the products' concentration profile during the reforming step of the cycle showed that the reformate gas evolves almost simultaneously with the introduction of the CH_4/steam feed, indicating that reforming reactions occur as soon as some metallic nickel is formed on the surface. In terms of stability, NiO/ZrO_2 exhibited an excellent stability with less than 2% relative decrease in conversion after 20 consecutive cycles. Deactivation of NiO/Al_2O_3 and $NiO/NiAl_2O_4$ was higher and equal to ~23% decrease in conversion for both OTMs. This loss of activity can be possibly attributed to low thermal stability of alumina and nickel aluminate supports when exposed to the high temperature of re-oxidation ($850\,^{\circ}C$) for extended periods of time.

Acknowledgments

This research was made possible by a grant (NPRP Grant No. 5-420-2-166) from the Qatar National Research Fund (a member of Qatar Foundation). The statements made herein are solely the responsibility of the authors. Dr. P. Patsalas and Mr. N. Pliatsikas from the Physics Department of the Aristotle University of Thessaloniki are gratefully acknowledged for the XPS measurements.

References

[1] P. Kruger, Appropriate technologies for large-scale production of electricity and hydrogen fuel, Int. J. Hydrogen Energy 33 (2008) 5881–5886, http://dx.doi.org/10.1016/j.ijhydene.2008.08.001.
[2] Y. Matsumura, T. Nakamori, Steam reforming of methane over nickel catalysts at low reaction temperature, Appl. Catal. A: Gen. 258 (2004) 107–114, http://dx.doi.org/10.1016/j.apcata.2003.08.009.
[3] E. Kikuchi, S. Uemiya, T. Matsuda, Hydrogen production from methane steam reforming assisted by use of membrane reactor, in: Nat. Gas Convers., 1991, pp. 509–515.
[4] C.S. Patil, M. Sint Annaland, J.A.M. Kuipers, Experimental study of a membrane assisted fluidized bed reactor for H-2 production by steam reforming of CH_4, Chem. Eng. Res. Des. 84 (2006) 399–404, http://dx.doi.org/10.1205/cherd05028.
[5] A.M. Dehkordi, C. Savari, M. Ghasemi, Steam reforming of methane in a tapered membrane-assisted fluidized-bed reactor: modeling and simulation, Int. J. Hydrogen Energy 36 (2011) 490–504, http://dx.doi.org/10.1016/j.ijhydene.2010.10.052.
[6] L. Barelli, G. Bidini, F. Gallorini, S. Servili, Hydrogen production through sorption-enhanced steam methane reforming and membrane technology: a review, Energy. 33 (2008) 554–570, http://dx.doi.org/10.1016/j.energy.2007.10.018.
[7] M. Broda, V. Manovic, Q. Imtiaz, A.M. Kierzkowska, E.J. Anthony, C.R. Müller, High-purity hydrogen via the sorption-enhanced steam methane reforming reaction over a synthetic CaO-based sorbent and a Ni catalyst, Environ. Sci. Technol. 47 (2013) 6007–6014, http://dx.doi.org/10.1021/es305113p.
[8] C.S. Martavaltzi, A.A. Lemonidou, Hydrogen production via sorption enhanced reforming of methane: development of a novel hybrid material-reforming catalyst and CO_2 sorbent, Chem. Eng. Sci. 65 (2010) 4134–4140, http://dx.doi.org/10.1016/j.ces.2010.04.038.
[9] H.R. Radfarnia, M.C. Iliuta, Hydrogen production by sorption-enhanced steam methane reforming process using CaO-Zr/Ni bifunctional sorbent-catalyst, Chem. Eng. Process. Process Intensif. 86 (2014) 96–103, http://dx.doi.org/10.1016/j.cep.2014.10.014.
[10] F.-X. Chiron, G.S. Patience, S. Rifflart, Hydrogen production through chemical looping using $NiO/NiAl_2O_4$ as oxygen carrier, Chem. Eng. Sci. 66 (2011) 6324–6330, http://dx.doi.org/10.1016/j.ces.2011.03.060.
[11] L.F. de Diego, M. Ortiz, F. García-Labiano, J. Adánez, A. Abad, P. Gayán, Hydrogen production by chemical-looping reforming in a circulating fluidized

bed reactor using Ni-based oxygen carriers, J. Power Sources 192 (2009) 27–34, http://dx.doi.org/10.1016/j.jpowsour.2008.11.038.
[12] B. Jiang, B. Dou, Y. Song, C. Zhang, B. Du, H. Chen, et al., Hydrogen production from chemical looping steam reforming of glycerol by Ni-based oxygen carrier in a fixed-bed reactor, Chem. Eng. J. 280 (2015) 459–467, http://dx.doi.org/10.1016/j.cej.2015.05.120.
[13] H. Zhao, L. Guo, X. Zou, Chemical-looping auto-thermal reforming of biomass using Cu-based oxygen carrier, Appl. Energy (2015), http://dx.doi.org/10.1016/j.apenergy.2015.04.093.
[14] K. Zhao, F. He, Z. Huang, A. Zheng, H. Li, Z. Zhao, Three-dimensionally ordered macroporous $LaFeO_3$ perovskites for chemical-looping steam reforming of methane, Int. J. Hydrogen Energy 39 (2014) 3243–3252, http://dx.doi.org/10.1016/j.ijhydene.2013.12.046.
[15] F. García-Labiano, E. García-Díez, L.F. de Diego, A. Serrano, A. Abad, P. Gayán, et al., Syngas/H_2 production from bioethanol in a continuous chemical-looping reforming prototype, Fuel Process. Technol. 137 (2015) 24–30, http://dx.doi.org/10.1016/j.fuproc.2015.03.022.
[16] M.M. Hossain, H.I. de Lasa, Chemical-looping combustion (CLC) for inherent CO_2 separations – a review, Chem. Eng. Sci. 63 (2008) 4433–4451, http://dx.doi.org/10.1016/j.ces.2008.05.028.
[17] N.R. McGlashan, The thermodynamics of chemical looping combustion applied to the hydrogen economy, Int. J. Hydrogen Energy 35 (2010) 6465–6474, http://dx.doi.org/10.1016/j.ijhydene.2010.03.108.
[18] L.-S. Fan, L. Zeng, W. Wang, S. Luo, Chemical looping processes for CO_2 capture and carbonaceous fuel conversion – prospect and opportunity, Energy Environ. Sci. 5 (2012) 7254, http://dx.doi.org/10.1039/c2ee03198a.
[19] M. Rydén, P. Ramos, H_2 production with CO_2 capture by sorption enhanced chemical-looping reforming using NiO as oxygen carrier and CaO as CO_2 sorbent, Fuel Process. Technol. 96 (2012) 27–36, http://dx.doi.org/10.1016/j.fuproc.2011.12.009.
[20] A. Antzara, E. Heracleous, D.B. Bukur, A.A. Lemonidou, Thermodynamic analysis of hydrogen production via chemical looping steam methane reforming coupled with in situ CO_2 capture, Int. J. Greenh. Gas Control 32 (2015) 115–128, http://dx.doi.org/10.1016/j.ijggc.2014.11.010.
[21] A. Abad, J. Adánez, F. García-Labiano, L.F. de Diego, P. Gayán, J. Celaya, Mapping of the range of operational conditions for Cu-, Fe-, and Ni-based oxygen carriers in chemical-looping combustion, Chem. Eng. Sci. 62 (2007) 533–549, http://dx.doi.org/10.1016/j.ces.2006.09.019.
[22] J. Adánez, L.F. De Diego, F. García-Labiano, P. Gayán, A. Abad, J.M. Palacios, Selection of oxygen carriers for chemical-looping combustion, Energy Fuels 18 (2004) 371–377, http://dx.doi.org/10.1021/ef0301452.
[23] H.R. Forutan, E. Karimi, A. Hafizi, M.R. Rahimpour, P. Keshavarz, Expert representation chemical looping reforming: a comparative study of Fe, Mn, Co and Cu as oxygen carriers supported on Al_2O_3, J. Ind. Eng. Chem. 21 (2014) 900–911, http://dx.doi.org/10.1016/j.jiec.2014.04.031.
[24] M. Tang, L. Xu, M. Fan, Progress in oxygen carrier development of methane-based chemical-looping reforming: a review, Appl. Energy 151 (2015) 143–156, http://dx.doi.org/10.1016/j.apenergy.2015.04.017.
[25] K. Shah, B. Moghtaderi, T. Wall, Selection of suitable oxygen carriers for chemical looping air separation: a thermodynamic approach, Energy Fuels 26 (2012) 2038–2045, http://dx.doi.org/10.1021/ef300132c.
[26] L.F. de Diego, M. Ortiz, J. Adánez, F. García-Labiano, A. Abad, P. Gayán, Synthesis gas generation by chemical-looping reforming in a batch fluidized bed reactor using Ni-based oxygen carriers, Chem. Eng. J. 144 (2008) 289–298, http://dx.doi.org/10.1016/j.cej.2008.06.004.
[27] M. Rydén, A. Lyngfelt, T. Mattisson, Synthesis gas generation by chemical-looping reforming in a continuously operating laboratory reactor, Fuel 85 (2006) 1631–1641, http://dx.doi.org/10.1016/j.fuel.2006.02.004.
[28] T. Mattisson, A. Järdnäs, A. Lyngfelt, Reactivity of some metal oxides supported on alumina with alternating methane and oxygen – application for chemical-looping combustion, Energy Fuels 17 (2003) 643–651, http://dx.doi.org/10.1021/ef020151i.
[29] T. Mattisson, M. Johansson, A. Lyngfelt, The use of NiO as an oxygen carrier in chemical-looping combustion, Fuel 85 (2006) 736–747, http://dx.doi.org/10.1016/j.fuel.2005.07.021.
[30] P. Gayán, L.F. de Diego, F. García-Labiano, J. Adánez, A. Abad, C. Dueso, Effect of support on reactivity and selectivity of Ni-based oxygen carriers for chemical-looping combustion, Fuel 87 (2008) 2641–2650, http://dx.doi.org/10.1016/j.fuel.2008.02.016.
[31] M. Rydén, M. Johansson, A. Lyngfelt, T. Mattisson, NiO supported on Mg–ZrO_2 as oxygen carrier for chemical-looping combustion and chemical-looping reforming, Energy Environ. Sci. 2 (2009) 970, http://dx.doi.org/10.1039/b904370e.
[32] Q. Zafar, T. Mattisson, B. Gevert, Integrated hydrogen and power production with CO_2 capture using chemical-looping reforming redox reactivity of particles of CuO, Mn_2O_3, NiO, and Fe_2O_3 Using SiO_2 as a support, Ind. Eng. Chem. Res. 44 (2005) 3485–3496, http://dx.doi.org/10.1021/ie048978i.
[33] L. Silvester, A. Antzara, G. Boskovic, E. Heracleous, A.A. Lemonidou, D.B. Bukur, NiO supported on Al_2O_3 and ZrO_2 oxygen carriers for chemical looping steam methane reforming, Int. J. Hydrogen Energy 40 (2015) 7490–7501, http://dx.doi.org/10.1016/j.ijhydene.2014.12.130.
[34] V.G. Deshmane, S.L. Owen, R. Abrokwah, D. Kuila, Mesoporous nanocrystalline TiO_2 supported metal (Cu, Co, Ni, Pd, Zn, and Sn) catalysts: effect of metal–support interactions on steam reforming of methanol, J. Mol. Catal. A: Chem. (2015), http://dx.doi.org/10.1016/j.molcata.2015.07.023.
[35] J.M. Rynkowski, T. Paryjczak, M. Lenik, On the nature of oxidic nickel phases in NiO/γ-Al_2O_3 catalysts, Appl. Catal. A: Gen. 106 (1993) 73–82, http://dx.doi.org/10.1016/0926-860X(93)80156-K.
[36] G. Li, L. Hu, J.M. Hill, Comparison of reducibility and stability of alumina-supported Ni catalysts prepared by impregnation and co-precipitation, Appl. Catal. A: Gen. 301 (2006) 16–24, http://dx.doi.org/10.1016/j.apcata.2005.11.013.
[37] P. Kim, Y. Kim, H. Kim, I.K. Song, J. Yi, Synthesis and characterization of mesoporous alumina with nickel incorporated for use in the partial oxidation of methane into synthesis gas, Appl. Catal. A: Gen. 272 (2004) 157–166, http://dx.doi.org/10.1016/j.apcata.2004.05.055.
[38] C. Li, Y.-W. Chen, Temperature-programmed-reduction studies of nickel oxide/alumina catalysts: effects of the preparation method, Thermochim. Acta 256 (1995) 457–465, http://dx.doi.org/10.1016/0040-6031(94)02177-P.
[39] Q.G. Yan, W.Z. Weng, H.L. Wan, H. Toghiani, R.K. Toghiani, C.U. Pittman, Activation of methane to syngas over a Ni/TiO_2 catalyst, Appl. Catal. A: Gen. 239 (2003) 43–58, http://dx.doi.org/10.1016/S0926-860X(02)00351-4.
[40] S.W. Ho, C.Y. Chu, S.G. Chen, Effect of thermal treatment on the nickel state and CO hydrogenation activity of titania-supported nickel catalysts, J. Catal. 178 (1998) 34–48, http://dx.doi.org/10.1006/jcat.1998.2102.
[41] R. Molina, G. Poncelet, α-Alumina-supported nickel catalysts prepared from nickel acetylacetonate: a TPR study, J. Catal. 173 (1998) 257–267.
[42] A. Antzara, E. Heracleous, A.A. Lemonidou, Improving the stability of synthetic CaO-based CO_2 sorbents by structural promoters, Appl. Energy 156 (2015) 331–343, http://dx.doi.org/10.1016/j.apenergy.2015.07.026.
[43] A. Al-Ubaid, E.E. Wolf, Steam reforming of methane on reduced non-stoichiometric nickel aluminate catalysts, Appl. Catal. 40 (1988) 73–85, http://dx.doi.org/10.1016/S0166-9834(00)80427-3.
[44] J.R. Rostrup-Nielsen, Activity of nickel catalysts for steam reforming of hydrocarbons, J. Catal. 31 (1973) 173–199, http://dx.doi.org/10.1016/0021-9517(73)90326-6.
[45] J. Rostrup-Nielsen, Mechanisms of carbon formation on nickel-containing catalysts, J. Catal. 48 (1977) 155–165, http://dx.doi.org/10.1016/0021-9517(77)90087-2.
[46] C. Bartholomew, Mechanism of catalyst deactivation, Appl. Catal. A: Gen. 212 (2001) 17–60, http://dx.doi.org/10.1016/S0926-860X(00)00843-7.
[47] C.H. Bartholomew, Catalysis reviews: science and reforming and methanation carbon deposition in steam reforming and methanation, Catal. Rev. Sci. Eng. 24 (1) (1982) 67–112, http://dx.doi.org/10.1080/03602458208079650.
[48] J.R. Rostrup-Nielsen, J. Sehested, J.K. Noerskov, Hydrogen and synthesis gas by steam- and CO_2 reforming, ChemInform 34 (2003), http://dx.doi.org/10.1002/chin.200317288.
[49] N.V. Parizotto, K.O. Rocha, S. Damyanova, F.B. Passos, D. Zanchet, C.M.P. Marques, et al., Alumina-supported Ni catalysts modified with silver for the steam reforming of methane: effect of Ag on the control of coke formation, Appl. Catal. A: Gen. 330 (2007) 12–22, http://dx.doi.org/10.1016/j.apcata.2007.06.022.
[50] V. Nichele, M. Signoretto, F. Menegazzo, A. Gallo, V. Dal Santo, G. Cruciani, et al., Glycerol steam reforming for hydrogen production: design of Ni supported catalysts, Appl. Catal. B: Environ. 111–112 (2012) 225–232, http://dx.doi.org/10.1016/j.apcatb.2011.10.003.
[51] K. Takehira, T. Ohi, T. Miyata, M. Shiraga, T. Sano, Steam reforming of CH_4 over Ni–Ru catalysts supported on Mg–Al mixed oxide, Top. Catal. 42–43 (2007) 471–474, http://dx.doi.org/10.1007/s11244-007-0227-6.
[52] R.V. Siriwardane, J.A. Poston Jr., E.P. Fisher, Interaction of hydrogen sulfide with $Zr_{0.92}Y_{0.08}O_{2-\delta}$/40% Ni cermet, Appl. Surf. Sci. 243 (2005) 40–54, http://dx.doi.org/10.1016/j.apsusc.2004.07.070.
[53] R. Shalvoy, P. Reucroft, B. Davis, Characterization of coprecipitated nickel on silica methanation catalysts by X-ray photoelectron spectroscopy, J. Catal. 348 (1979) 336–348, pii:002195177990126X.
[54] M.A. Nieva, M.M. Villaverde, A. Monzón, T.F. Garetto, A.J. Marchi, Steam-methane reforming at low temperature on nickel-based catalysts, Chem. Eng. J. 235 (2014) 158–166, http://dx.doi.org/10.1016/j.cej.2013.09.030.
[55] J. Rostrup-Nielsen, L.J. Christiansen, Concepts in Syngas Manufacture, 2011.
[56] R. Takahashi, S. Sato, T. Sodesawa, M. Yoshida, S. Tomiyama, Addition of zirconia in Ni/SiO_2 catalyst for improvement of steam resistance, Appl. Catal. A: Gen. 273 (2004) 211–215, http://dx.doi.org/10.1016/j.apcata.2004.06.033.
[57] P. Cho, T. Mattisson, A. Lyngfelt, Carbon formation on nickel and iron oxide-containing oxygen carriers for chemical-looping combustion, Ind. Eng. Chem. Res. 44 (2005) 668–676, http://dx.doi.org/10.1021/ie049420d.
[58] V. Dupont, A.B. Ross, I. Hanley, M.V. Twigg, Unmixed steam reforming of methane and sunflower oil: a single-reactor process for H_2-rich gas, Int. J. Hydrogen Energy 32 (2007) 67–79, http://dx.doi.org/10.1016/j.ijhydene.2006.06.033.

Please cite this article in press as: A. Antzara, et al., Activity study of NiO-based oxygen carriers in chemical looping steam methane reforming, Catal. Today (2015), http://dx.doi.org/10.1016/j.cattod.2015.10.027